Light Transmittance of Mahogany Wood Treated with 20% Hydrogen Peroxide Solution

Jasmina Popovic,[a] Srdjan Svrzic,[a,*] Milica Gajic,[a] Slavica Maletic,[b] Vladimir Dodevski,[c] Milanka Djiporovic-Momcilovic,[a] Sanja Krstic,[c] and Mladjan Popovic [a]

There is an increased research interest in methods for transparent wood production and its use. Wood transparency could be achieved by its delignification followed by an impregnation process with polymers having proper optical properties. However, delignification processes are mainly time consuming and not environmentally friendly. The possibility of treating mahogany wood (*Swietenia macrophylla* King) with 20% hydrogen peroxide for 70, 100, 135, and 170 min at 103 °C is presented in this research. According to the treatment duration, lignin content decreased 40 to 94% relative to its initial content in the control samples, whilst the cell structure remained intact. Due to the light scatter effect, caused mainly by wood tissue structure, the direct optical transmittance of treated samples in the visible light spectrum (400 to 800 nm) was less than 40%. Simultaneously, the total optical transmittance of samples treated for 100 and 135 min reached values between 70 to 80% with high values of the haze at approximately 30 and 60%. Optical transmittance in the visible spectrum area of the samples treated for 170 min was from 45 to 80% and the haze from 25 to 45%.

DOI: 10.15376/biores.17.4.5919-5935

Keywords: Transparent wood; 20% Hydrogen peroxide; Lignin content; Optical transmittance; Haze

*Contact information: a: Department of Wood Science and Technology, University of Belgrade- Faculty of Forestry, 11000 Belgrade, Serbia; b: University of Belgrade-Faculty of Physics, 11000 Belgrade, Serbia; c: Department of Materials, Institute of Nuclear Sciences, Vinca, University of Belgrade-National Institute of the Republic of Serbia, Belgrade 11001 Serbia; *Corresponding author: srdjan.svrzic@sfb.bg.ac.rs*

INTRODUCTION

Despite the fact that wood use is vast, new possibilities of processing and implementation of this renewable natural material are constantly being researched. In previous decades, numerous researchers studied the possibilities of modifications of certain wood properties, resulting in new products with enhanced characteristics (Rowell 2005; Hill 2006). However, until recent years, there was little attention given to optical properties and their modification. During the light-wood interaction, depending on light wavelength and wood density, chemical composition, and anatomic direction, the combination of reflection, refraction, absorption, and transmission of light is occurring (Li *et al.* 2017a). Lignin plays a predominant role in light absorption in wood (80 to 90%), whilst the carbohydrates contribute 5 to 20%, and the extractives contribute approximately 2%. Along with the absorption, on the boundary surfaces between cell wall and surrounding media, the refraction of light occurs in the form of scattering (Li *et al.* 2017a). Recently, optical property modification methods are proposed to improve optical transmittance of wood.

The transparent products in the form of the film based on nano-sized or micro-sized cellulose fibres with high optical transmittance (80 to 90%) have been known for some time (Zhu *et al.* 2016a). However, these products are not comparable with genuine wood tissue in the manner of hierarchical structure and wood fiber orientation, and this limits their utilization wherever the more complex structure is needed (Li *et al.* 2017a). New procedures are being proposed for transparent wood with preserved cell structure production as well as its application. Thanks to the unique hierarchical structure, as well as pretty good mechanical, optical, and thermal properties, the possibility of transparent wood with preserved structure to be utilized as energy efficient and eco-friendly construction material has been taken into serious consideration, especially for the roof and window manufacturing sectors (Li *et al.* 2016a: Yaddanapudi *et al.* 2017), as well as improving solar cell efficiency (Zhu *et al.* 2016b).

Through the introduction of magnetic (Fe_3O_4), luminescent (Si or CdSe), or infrared (IR) absorbing (Cs_xWO_3 or W/VO_2) nanoparticles or disposing electrochromic layers onto the transparent wood, a great spectrum of possible applications widens, such as in heat-shielding buildings and windows (Yu *et al.* 2017), smart windows (Lang *et al.* 2018; Wang *et al.* 2019; Zhang *et al.* 2020), light sources, luminescent building elements or design furniture (Li *et al.* 2017c; Fu *et al.* 2018), magnetic switches and electromagnetic interference shielding (Gan *et al.* 2016, 2017; Li *et al.* 2018a), and optoelectronics (Zhu *et al.* 2016b).

For the purpose of achieving wood transparency it is necessary to decrease absorption and scattering of light, which includes two stages. The first stage involves removing the lignin and other colored components (mostly polyphenols) from the wood, which leads to a decrease in light absorbance (Li *et al.* 2017a). The second stage targets the light scattering that occurs at boundary surfaces.

Delignification could be achieved through the chemical treatments that selectively target lignin component of wood tissue. In a study aimed at easier wood structure, Fink (1992) treated various wood samples with 5% aqueous solution of sodium hypochlorite (NaClO) during 1 to 2 days, obtaining the first samples of transparent wood (Li *et al.* 2017a). The long term (6 to 10 h) wood treatment with 1% potassium chlorite ($NaClO_2$) in acetate puffer solution (pH 4.6) along with heating (45 to 80 °C) decreases lignin content from 25% to approximately 3% (Li *et al.* 2017a, 2018b; Fu *et al.* 2018). The delignification process also could be attained by using 2.5 M NaOH and 0.4 M Na_2SO_3 at boiling temperature for 12 h, and subsequent treatment with 2.5 M H_2O_2, reaching total bleaching of the samples (Zhu *et al.* 2016a).

A decreasing in light scattering on boundary surfaces could be gained by filling the wood microstructure with a proper polymer that has a refraction index similar to that of delignified wood. Simultaneously, these polymers take the adhesive role of removed lignin (Li *et al.* 2017a, 2018a). The most commonly used polymers are polymethyl acrylate (PMMA) with refraction index of $I_r = 1.49$ and epoxy resin with $I_r = 1.50$ (Li *et al.* 2017b). Thus, delignified wood impregnated with polymer results in a transparent wood sample with transmittance of about 80% and the haze of about 75%, depending on wood species and type of applied polymer (Li *et al.* 2017a).

All procedures mentioned above are time consuming and environmentally unsuitable (Li *et al.* 2017a). Hydrogen peroxide is a well-known treatment for the bleaching of the pulp (Ramos *et al.* 2008). In the bleaching process, mild conditions are used in terms of low peroxide concentrations, temperatures from 40 to 60 °C or from 60 to 80 °C for 1 to 4 h, in the presence of sodium silicate, which had the role of stabilizer and puffer

(Gellerstedt 2007; Ramos *et al.* 2008). Under these mild reaction conditions, peroxide has little or no delignification effect, which leads to structural modification of the lignin with removal of the chromophore groups without significant degradation (Ramos *et al.* 2008). Through the use of the solution containing deionized water, sodium silicate (3.0 wt%), sodium hydroxide (3.0 wt%), magnesium sulfate (0.1 wt%), diethylenetriaminepentaacetic acid (DTPA) (0.1 wt%), and H_2O_2 (4.0 wt%) at 70 °C after 6 h, a brightness around 80% for 1.5-mm-thick samples of pine, birch, balsa, and ash, was achieved (Li *et al.* 2017b). After this procedure about 80 wt% of lignin of genuine wood structure was preserved. However, in harsher reaction conditions in terms of temperature (100 °C) and in the absence of silicates, hydrogen peroxide has the ability of oxidative delignification (Gellerstedt 2007; Ramos *et al.* 2008). Hydrogen peroxide as oxidative reagent efficiently oxidizes aromatic lignin rings and partially hemicelluloses, whilst the cellulose remains resistant (Miron and Ben-Ghedalia 1982). Through the series of oxidative reactions, with complex reaction mechanism, depolymerization and dissolution of the lignin occurs (Kalliola *et al.* 2011). Radicals originating from H_2O_2 attack lateral chains of lignin structure, causing fragmentation of its macrostructure, and thus forming a variety of low molecular weight compounds (Selig *et al.* 2009). Hydrogen peroxide treatment of the wheat straw and corn stalks removes almost 60% of the lignin and majority of hemicelluloses from these materials (Gould 1984). The treatment with alkaline hydrogen peroxide (pH = 11.5) at 30 °C solubilized approximately 50% of the lignin and most of the hemicelluloses (Azzam 1989).

In addition to hydrogen peroxide capability of delignification, it is easy to transport, store, and use, and its non-toxicity and non-toxicity of its reaction products, makes it environmentally acceptable and safe (Ramos *et al.* 2008). Furthermore, the possible use of hydrogen peroxide to obtain transparent wood was investigated in this paper.

EXPERIMENTAL

Mahogany wood (*Swietenia macrophylla* King) was used for the purpose of this research in the form of radial cut veneer with 20 mm (radially oriented) × 70 mm (axially oriented) dimensions and the thickness of 0.5 ± 0.02 mm.

Fabrication of Transparent Wood

The process of sample treatment was conducted in two phases: delignification and impregnation.

During the process of delignification, the samples were treated with 20% water solution of hydrogen peroxide (ZORKA Pharma-Hemija d.o.o. Šabac, Serbia) at boiling temperature of 103.41 °C during three different time intervals for the different sample groups (70, 100, and 135 min, further TW70, TW100, and TW135, respectively) and for the fourth group until reaching the total bleach effect after about 170 min (TW170). The totally bleached samples (TW170) were subjected to defibrillation, thus making their preparation with conserved structure extremely difficult. The measured pH value of prepared peroxide solution was 5.5. Then the treatment samples were carefully rinsed with distilled water. The samples of each treated and untreated groups were mechanically chopped to the approximately 1 mm particle size and air dried. The rest of the samples were kept in 96% v/v ethanol (ZORKA Pharma-Hemija d.o.o. Šabac, Serbia) before being impregnated.

The impregnation process was performed with epoxy resin (105 Epoxy Resin and 205 Hardener, West System, Gougeon Brothers, Inc., Bay City, MI, USA) with refraction index (I_r) of 1.5, which is close to the value of I_r of cellulose and hemicelluloses (1.53) (Li *et al.* 2017a). The viscosity of epoxy resin (mixed) was 975 cP (at 22ºC) defined by ASTM D2393 according to manufacturer specification. Epoxy resin was prepared according to manufacturer instructions. The sets of the two microscope slides were set on the scale to tare the scale. In this way it was possible to measure the exact weight of resin applied. The prepared epoxy resin was applied in the thin layer on the microscope slides. Afterwards the samples of mahogany veneer were placed on coated microscope slides, coated again with the same amounts of epoxy resin, and finally covered with another set of microscope slides. Control samples without mahogany veneer and with the same amount of resin were prepared in the same manner. The prepared samples were wrapped in aluminum foil, left at room temperature (21 ± 3 °C), and exposed to pressure of about 14.7 kPa during the period of 24 h to harden the resin.

Characterization

The moisture content was determined gravimetrically, according to the TAPPI T264 cm-97 (1997) method. Samples mass loss (*ML*) during the delignification treatment was determined as the dry mass difference of the samples before (m_{nt}) and after the treatment (m_{tr}) according to Eq. 1:

$$ML = \frac{m_{nt} - m_{tr}}{m_{nt}} \times 100 \ (\%) \quad (1)$$

The extractives content soluble in organic solvents in treated and control samples was determined by continuous extraction with ethanol-toluene mixture (1:2 v/v) in the Soxhlet extractor for 8 h as per ASTM D1107-96 (1996). The Klason modified method (per TAPPI T 222 om-02 (2006)) was performed to ascertain the lignin content.

The analysis of characteristic functional groups for control and treated samples was investigated using a Fourier transform infrared (FTIR) spectrometer (PerkinElmer, Inc., Waltham, MA, USA). Spectra were recorded in the range from 400 to 4000 cm^{-1} and at 4 cm^{-1} resolution.

For the aim of morphology examination, impregnated samples were observed and photographed by the system consisting of a Leica DMRB microscope with magnification of 20 times and Leica Wetzlar, Germany 541000 camera using supporting software Leica LAS (v4.13, Leica, Wetzlar, Germany).

Optical Properties Examination

For the visual characterization, optical transmittance samples were placed on printed text "*Is this wood?*" (Fig. 4), which was printed on the layer beneath the samples with Calibri font size 28 and then photographed.

For the purpose of anisotropy of optical properties, the samples were placed on the net printed background and photographed at a distance of 5 mm.

Optical Transmittance Measurements

Optical transmittance of monochromatic light, as well as haze, were determined with a wavelength of 633 nm and visible electro-magnetic (EM) spectral area with wavelengths from 400 to 800 nm. For all optical experimental procedures, samples were positioned in such manner that light impacted them normally to the radial sample surface and consequently normally to fiber orientation.

Optical Transmittance Measurements of Monochromatic Light

Monochromatic light transmittance measurements of investigated samples were based upon the photoelectric effect. The optical apparatus layout is presented in Fig. 1, which consists of the light source (W), lenses S_1 and S_2 for the setup (a) and lenses S_1, S_2, and S_3 for the setup (b) (as presented in Fig. 1), and photoelectric detector (D). The monochromatic light source was a He-Ne laser generator (Iskra, Kranj, Slovenia) with power of 2 mW, which emits a continuous monochromatic light beam with the wavelength of 633 nm. The photoelectric detector was photo-voltage cell (General Electric 88X565 GE Type PV-1, Boston, MA, USA), and it was attached to 0 to 100 V measuring range voltmeter with 2 V accuracy range (Zavod Elektrodelo, Leningrad, SSSR). The detector was placed orthogonally to the axis of collimated monochromatic light beam. The narrowed (2 mm in radius) and expanded (25 mm in radius) collimated monochromatic light beams were directed to the samples (U) that were positioned in front of the detector. The voltage generated in detector was proportional to optical transmittance and recorded on the voltmeter. The optical transmittance was measured for three samples from each specimen group at three different positions at each sample.

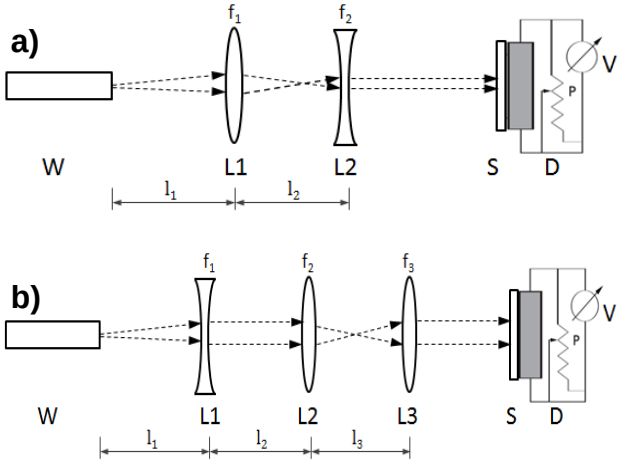

W – Source of monochromatic light (633 nm); S – sample; D – photo-detector; L1 – converging lens (f_1 = 40.5 cm); L2 – diverging lens (f_2 = -35 cm); l_1 = 186 cm; l_2 = 16.5 cm

W – Source of monochromatic light (633 nm); S – sample; D – photo-detector; L1 – diverging lens (f_1 = -21 cm); L2 – converging lens (f_2 = -16 cm; L3 – converging lens (f_2 = 25 cm); l_1 = 40 cm; l_2 = 212 cm; l_3 = 42 cm

Fig. 1. Optical transmittance apparatus layout a) with narrowed (D = 2 mm) and b) expanded (D = 25 mm) collimated monochromatic light beam

Optical Transmittance and Haze Measurement of Visible EM Spectral Area

There are two important physical parameters that determine optical properties of optically transparent wood: optical transmittance and haze. The optical transmittance refers to the ratio of the light energy transmitted, which includes scattered light, and the total incidence light energy. The haze is described as the relative amount of scattered light that deviates by more than a spatial angle of 2.5° from incidence light beam direction as per the

ASTM D1003-00 (2000) standard. Haze results in information loss, *i.e.*, decreasing the sharpness of image observed through wood samples.

Direct optical transmittance (DOT) and absorbance were measured using a spectrophotometer (Shimadzu UV-Vis-NIR 3600/3100 Series, Kyoto, Japan). Total optical transmittance (TOT) and haze were measured by the same apparatus with an integrated sphere. All measurements took place within visible EM spectrum (400 to 800 nm) and with the sampling interval of 1 nm. The haze measurement was recorded following the standard method for haze transparent plastics ASTM D1003-00 (2000). The haze was calculated according to Eq. 2,

$$H = \frac{T_d}{T_t} = \left(\frac{T_4}{T_2} - \frac{T_3}{T_1} \right) \times 100\% \quad (2)$$

where T_t is total transmittance (%) and T_d is transmittance of diffused light (%); T_1 is reference transmittance (%) – measurements of light intensity without specimen and with the white light standard placed; T_2 is light transmitted by sample (%) – measurements of light intensity with sample located at the input port of the sphere and white standard placed; T_3 is light scattered by instrument (%) – measurements of light intensity without the sample and a light trap replacing the white standard, and T_4 is light scattered by instrument and specimen (%) – measurements of light intensity with the sample and the light trap as per the ASTM D1003-00 (2000) standard.

RESULTS AND DISCUSSION

Chemical Composition and Mass Loss

Results for mass loss, lignin, and extractives content for control and treated samples are presented in Fig. 5. Porous wood structure permits diffusion of 20% solution of H_2O_2 into the interior of the samples, making chemical reactions possible, and thus resulting in alteration of the genuine chemical composition. The treatment resulted in mahogany wood losing between 17.9 and 58.8% of its starting mass, for TW70 and TW170, respectively, indicating noticeable decomposition of structural chemical components during the treatment, namely lignin. Results presented in Fig. 2 show that peroxide treatment strongly decreased the lignin content in all treated samples. Although under mild reaction conditions (lower temperatures, lower peroxide concentrations, and shorter reaction times) peroxide has a minor delignification effect, severe treatment conditions, such as the higher peroxide concentrations without adding the silicate, temperatures of 80 to 100 °C for a 1 to 2 h period of time, lead to serious delignification (30 to 40%) (Gellerstedt 2007; Ramos *et al.* 2008). At high temperatures at approximately 100 °C in peroxide system, nucleophilic cleavage of β-O-4 lignin substructures and lateral chain fragmentation is possible (Gellerstedt 2007). Generally, β-O-4 ether bonds comprise approximately 50% of all bonds in macromolecular structure of lignin (Fengel and Wegener 1984) and breaking these bonds could lead to a noticeable degree of delignification, which agrees with presented results. Furthermore, according to the results obtained, the increase of treatment duration decreased the lignin content. The initial lignin content of 38.3% decreased to 22.7% for TW70 and 2.19% for TW135. The latter showed a 94% decrease in lignin content, indicating high degree enactment of delignification reactions in such reaction system.

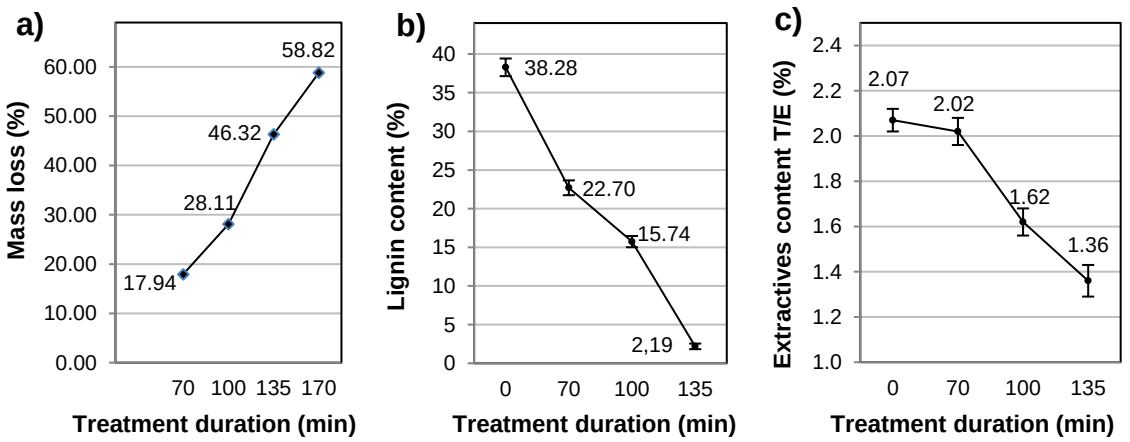

Fig. 2. Mass loss (a), lignin content (b), and extractives content (ethanol/toluene) (c) in mahogany wood treated with 20% hydrogen peroxide; 0 min – untreated samples

The dissolution of extractives in the reaction mixture also occurs during the treatment. This was noticeable because the ethanol/toluene soluble extractives content went from an initial value of 2.07% to 1.36% for 135 min treatment duration.

However, the total mass loss of 46.3% after 135 min and 58.3% after 170 min overwhelmed the sum of partial mass contents of lignin and extractives of untreated samples, 38.3% and 2.1%, respectively. This indicates that the process of decomposition of constituent polysaccharide compounds of wood occurs along with delignification and dissolution of extractives. The radicals present in the peroxide system, besides lignin oxidation, to a certain degree contribute to oxidation of polysaccharides as well (Gellerstedt 2007). In the conditions of oxidative delignification, "pilling" reactions occur on polysaccharides that lead to its depolymerization (Sjöström 1993). Moreover, the reaction of breaking glycosidic bonds in amorphous cellulose areas is also present (Stevanović-Janežić 1993). All reactions mentioned additionally contributed to the high mass loss during the treatment.

FTIR Spectroscopy

FTIR spectroscopy plays an important role for wood chemical structure change analysis. The FTIR spectra of untreated (NT) and treated mahogany wood after 70 min (TW70), 100 min (TW100), and 135 min (TW135) are presented in Fig. 3.

The spectrum of the control sample exhibits characteristic absorption peaks, such as O−H stretching vibration at 3331 cm^{-1} and C−H stretching vibrations at 2888 cm^{-1}. The strong absorption at these wavelengths indicates a huge presence of hydroxyl groups and many C−H bonds in the major component structure of biomass: cellulose, hemicelluloses, and lignin (Zhuang *et al.* 2020).

Characteristic absorption peaks for structural chemical compounds of wood (cellulose, hemicelluloses, and lignin) are present in the fingerprint regions of wood spectra (1800 to 800 cm^{-1}):

- C=O stretching vibrations of acetyl (or COOH) groups in hemicelluloses and lignin at 1732 cm^{-1} (Bodirlau and Teaca 2009; Pucetaite 2012; Zhuang *et al.* 2020);
- C=C stretching vibrations of the aromatic ring in lignin related to unsaturated linkages near 1614 cm^{-1} (Pucetaite 2012; Moosavinejad *et al.* 2016);

- C=C-C aromatic skeletal stretching vibrations of the benzene ring in lignin at 1505 cm^{-1} (Faix 1992; Lewis *et al.* 1994; Gelbrich *et al.* 2012);
- CH_2 scissoring vibration in lignin (Pandey 1999) and C-H asymmetric bending vibrations of CH_3 from methoxyl groups in lignin at 1455 cm^{-1} (Lionetto *et al.* 2012; Moosavinejad *et al.* 2016);
- C–H deformation and CH_2 symmetric bending vibration in hemicelluloses and cellulose near 1420 cm^{-1} (Traoré *et al.* 2018; Zhuang *et al.* 2020)
- C−H bending and C-H stretching in CH_2 in cellulose, hemicellulose, and lignin (aliphatic C-H stretching in methyl and phenolic alcohol) at 1370 cm^{-1} (Zhuang *et al.* 2020);
- CH_2 wagging in cellulose and hemicelluloses and the C-O stretching of C_5 substituted aromatic units, such as syringyl and condensed guaiacyl units, were assigned at 1317 cm^{-1} (Zhuang *et al.* 2020);
- C−O stretching vibrations of the acetyl groups in hardwood xylan (hemicelluloses) and syringyl ring (lignin) at 1232 cm^{-1} (Pandey and Pitman 2003; Moosavinejad *et al.* 2016);
- C−O−C ether bond (ring vibration) of carbohydrates (cellulose and hemicelluloses) and C-O stretching vibrations of primary alcohol in cellulose and hemicelluloses (dominated by ring vibration of carbohydrates) at 1026 cm^{-1}, and (Faix 1992; Pucetaite 2012);
- C−H in-plane symmetric vibration of carbohydrates; C-O-C stretching deformation of glucose ring in cellulose at 898 cm^{-1} (Lionetto *et al.* 2012; Pucetaite 2012).

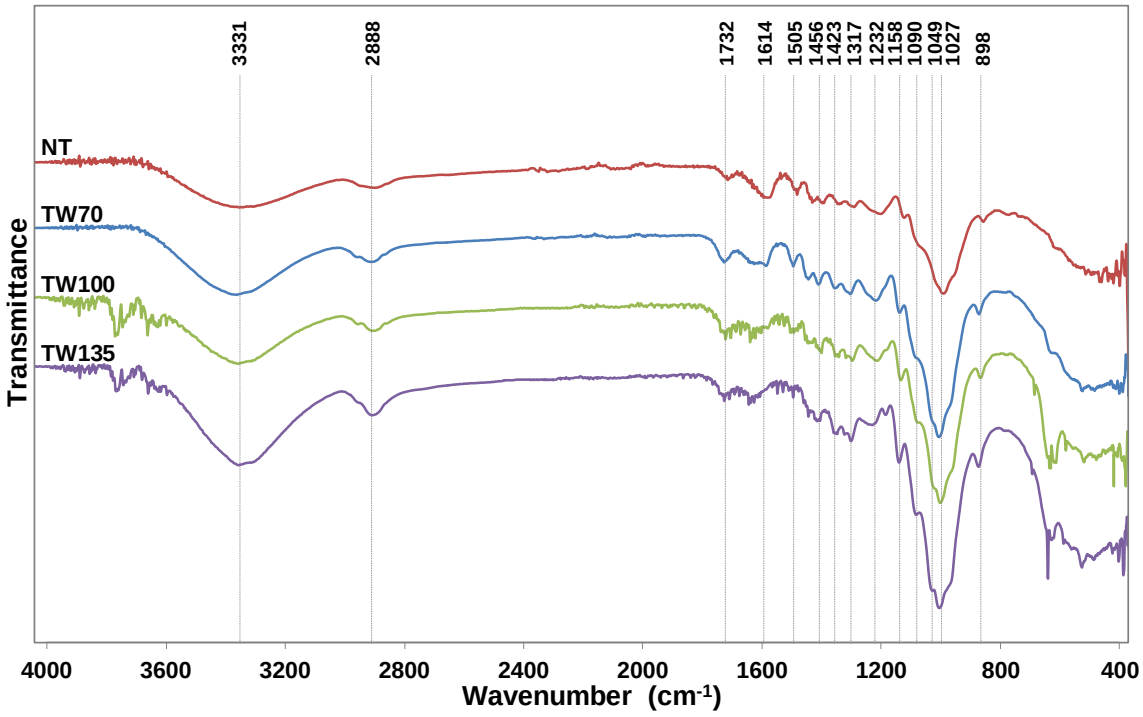

Fig. 3. FTIR spectra of NT and treated mahogany samples: TW70, TW100, and TW135

The FTIR spectra of treated samples for different treatment durations reflected changes in chemical structure that occurred during the treatment (Fig. 3). The lignin characteristic bands' intensity (at 1614 cm^{-1} and 1505 cm^{-1}) decreased with prolonged treatment duration, which goes along with previously determined lignin content reduction. The peak that corresponds to C=C stretching vibrations of the aromatic ring in lignin for TW70 shifted to 1594 cm^{-1} compared to 1614 cm^{-1} for NT. For the other treated samples this peak was not noticed.

Contrastingly, as expected, the characteristic peaks for carbohydrate components became more intense in the FTIR spectra of the treated samples. This was particularly emphasized in the 1200 to 890 cm^{-1} wavelength area, which is the polysaccharide region (Faix *et al.* 1991; Naumann *et al.* 1991). The characteristic bands for asymmetric stretching of C−O and C−C at 1158 cm^{-1} (Pucetaite 2012; Moosavinejad *et al.* 2016) and the asymmetric stretching of C−O−C at 1100 (1090) cm^{-1} (Pucetaite 2012), as well as stretching vibrations of C−O and C−C (Pandey 1999; Pucetaite 2012) at 1060 cm^{-1} in cellulose and hemicelluloses, are present in this area. These bands, as peaks at 1024 cm^{-1} and 898 cm^{-1}, were more expressive on FTIR spectra of treated samples, indicating an increased amount of carbohydrate components. Due to the delignification, lignin absorption at 1232 cm^{-1} decreased, causing the appearance of 1200 cm^{-1} peak, which could be attributed to ring vibration of carbohydrates at 1160 to 1197 cm^{-1} (Pucetaite 2012; Naumann *et al.* 1991). Simultaneously, on FTIR spectra of samples treated for TW100 and TW135, a decrease of peak intensity at 1732 cm^{-1}, which corresponds to acetyl groups in hemicelluloses, was noticed. The same peak is also linked to the lignin, illustrating that besides delignification, for the prolonged treatment duration, the process of hemicelluloses degradation is also present.

Samples Morphology and Visual Transparency

Macroscopic (a) and microscopic (b) images of control and treated samples of mahogany wood after epoxy resin impregnation are shown in Fig. 4. The images of NT and TW70 are dark brown, showing no transparency according to the visibility of the text ("*Is this wood?*"). This can be attributed to the high presence of the phenolic polymer – lignin – causing strong absorption in visible area of EM spectrum, thus resulting in the dark brown color. The TW100 samples were less dark, performing remarkably better transparency. The text behind the sample is legible but blurred. Further treatment extension resulted in less lignin in the samples whilst the color became lighter. The TW135 samples had a light ocher color and exhibited much better transparency, resulting in clear text visibility. Almost complete absence of any coloration could be detected for TW170 samples, resulting in almost perfect visibility of the text and therefore high optical transmittance.

The microscopic images of the samples, both treated and untreated, show clearly preserved wood texture with a highly arranged structure consisting of a great number of cells with different dimensions, shapes, and orientation (Fig. 5). Most of them are axially orientated fiber cells. Optical microscope images (Fig. 5) with 20 times magnification depict clearly preserved cell structure of the wood: mechanical fibers (libriform fibers) and parenchyma cells (axial parenchyma).

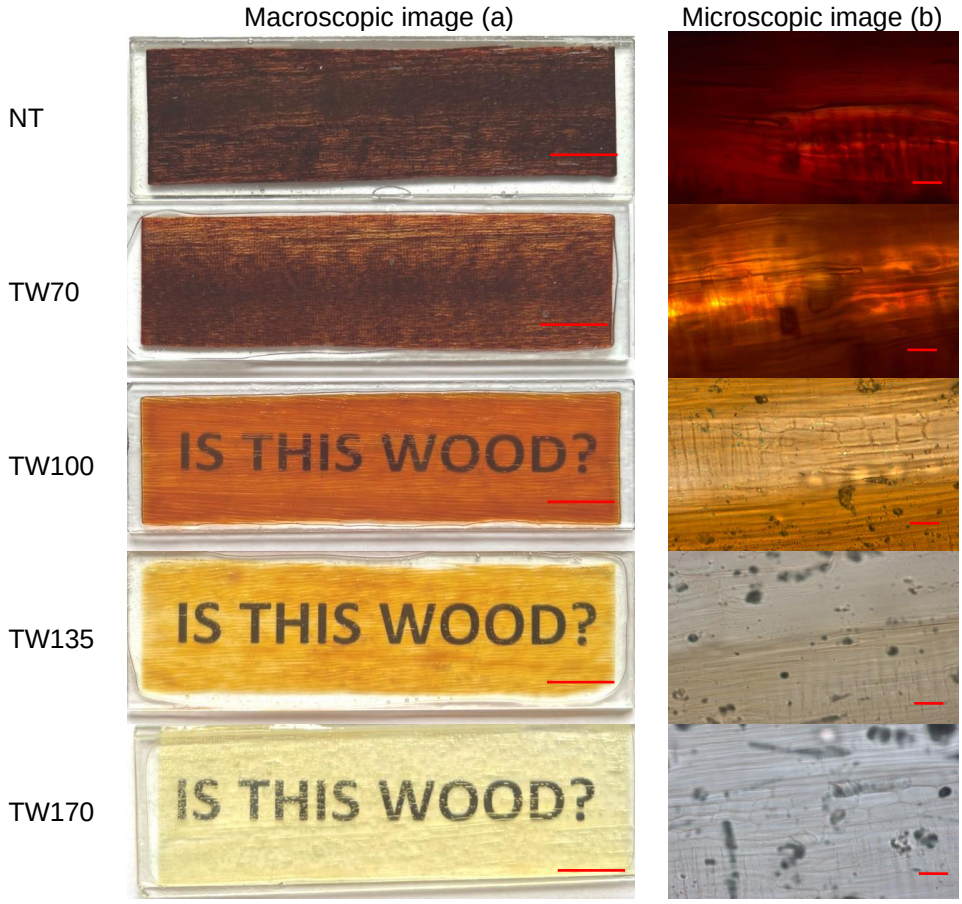

Fig. 4. Macroscopic, scale bar = 1 cm (a) and microscopic, scale bar = 100 µm (b) images of NT and treated samples of mahogany wood impregnated with epoxy resin

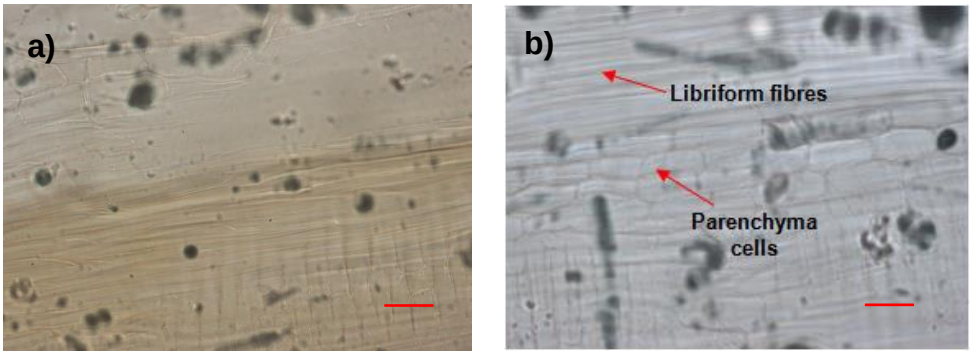

Fig. 5. Microscopic images of mahogany wood samples treated with 20% hydrogen peroxide a) TW135 and b) TW170 (magnification 20 x), scale bar = 100 µm

Although the cell structure of treated samples was almost completely preserved it cannot be denied that the lignin removal, as well as a certain amount of the other constituent compounds of the cell walls, leads to formation of the micro cavities in the cell walls. After the delignification of balsa wood the volume of the nano-pores increased, but the cell structure and cell orientation remained intact. The specific surface increased from 1.2 m^2/g to 19.8 m^2/g (Li *et al.* 2016b). The increase in porosity and specific surface could have the

positive effect on samples impregnation with resin after the delignification process (Li *et al.* 2016b).

Optical Transmittance of Monochromatic Light

During the passage of monochromatic light through some transparent matter, due to the light-matter interaction, a light energy loss occurs as well as the intensity drop of transmitted light. This interaction, in the form of reflection, dissipation, and absorption, depends on the light wavelength and physical-chemical nature of the matter. A photoelectric effect is responsible for generating a voltage signal that is correlated to the intensity of the transmitted light. Namely, when the light beam is passed through the investigated wood samples that are placed in front of the photo-detector, the generated voltage is proportional to the transmitted light intensity, *i.e.*, optical transmittance of the samples.

Figure 6a presents voltage values generated in photo-voltage cell in correlation with different treatment regimes and for the narrowed and expanded monochromatic light (633 nm) rays, after the specimens were treated with epoxy resin.

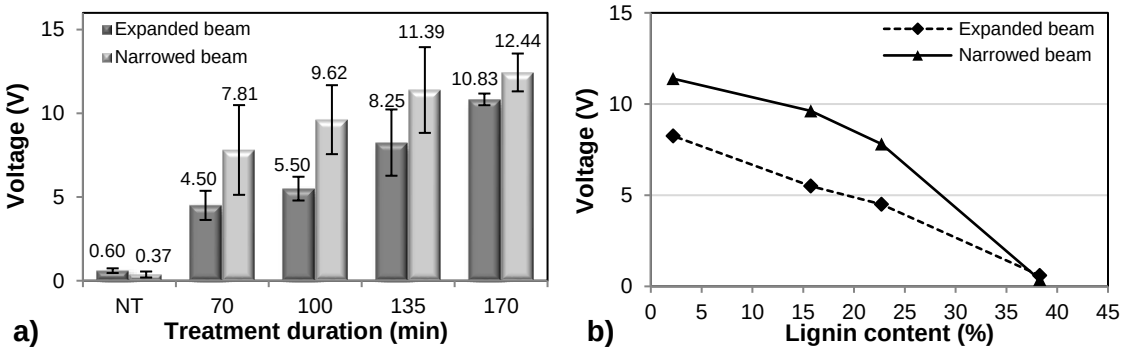

Fig. 6. Generated photo-voltage for different treatment duration (a) and for different lignin content (b) after monochromatic light (633 nm) transmitted through the samples

According to Fig. 6a, it is possible to note that the lowest values of generated voltage (0.37 and 0.60 V) corresponded to the untreated samples, indicating noticeable degree of absorption of laser light, supposedly related to the high lignin content (38.3%) as presented in Fig. 6b. The generated voltages noticeably increased in value in the treated samples, emphasizing the increase of optical transmittance of the sample after treatment. Along with the raising of the treatment duration, the values of measured voltage increased both for narrowed and expanded collimated laser beam. This is a result of the lift up of the transmitted light intensity, *i.e.*, decrease in light absorption that corresponds to elevated treatment duration. Generally, the chromophore structures present in lignin are responsible for most of the light absorption, as well as decreased light absorption of treated samples that could be related to the lignin displacement throughout the treatment process (Fig. 6b). According to previous studies (Dyer 2004; Tribulová *et al.* 2016), wood lignin contributes to light absorption 80 to 90%, which makes the previously shown relations quite expected.

Moreover, according to Fig. 6, the differences in the values of generated voltage were observed for narrowed and expanded collimated laser beams for the same groups of treated samples. These deviations could be explained by a light scattering effect on the boundary surfaces inside the samples. The expanded ray of light (25 mm) on its way through the sample would collide with a greater number of boundary surfaces (cell wall-

inter and intro cell space, cell wall-epoxy resin), at which due to different refraction indexes ($I_{Rcell\ wall}$ = 1.53; $I_{Repoxy\ resin}$ = 1.50 according to Li *et al.* 2017a) the scattering of light occurs. Furthermore, the scattering of light occurs inside the cell walls, resulting in lower values of generating voltage, *i.e.*, optical transmittance compared to the values obtained *via* narrowed collimated beam (2 mm).

For the narrowed collimated laser beam, high dissipation of measured voltage values at different positions across the same samples was noticed. The latter could be explained by inhomogeneity of wood tissue. The huge number of different cells varying in the shape and cell wall thickness, lumen radius, and chemical composition (Stevanović-Janežić 1993) are responsible for various values of optical paths and the light scatter causing differences in the intensity of transmitted light. Another reason for noticed results variation could be associated with different permeability of particular parts of wood samples, which would influence the diffusion of reactants in wood tissue and leading to uneven chemical reaction performance. Due to the previous considerations at the diverse samples, as well as at the same sample, the different degrees of delignification process could take place leading to uneven distribution of remaining lignin in the specimens.

This phenomenon was less obvious for the expanded collimated laser beam.

Optical Transmittance, Absorbance, and Haze in Visible Area of EM Spectrum

The results for optical transmittance, absorbance, and haze in visible EM spectrum (400 to 800 nm) for examined wood samples and epoxy resin are presented in Fig. 7. The DOT for NT samples and those for TW70 was negligibly small (Fig. 7a), and the absorbance was correspondingly high due to the remarkable lignin content (38.3 and 22.7%, for NT and TW70 samples, respectively). Through prolonged treatment duration, lignin content decreased accordingly, lowering the absorbance and lifting the transmittance properties of examined samples. The DOT of mahogany wood samples was the lowest near the UV spectral area and constantly increased with increasing light wavelength. Therefore, absorbance was greater at wavelengths below 550 nm, especially for samples treated for less time (Fig. 7b). The TW170 samples exhibited the highest DOT; however, they did not surpass the 33% transmittance value in the entire visible EM spectrum area.

The DOT in visible spectrum area measurements did not take into consideration scattered photons. For that reason TOT was measured using the integrating sphere, which gathers all scattered photons. The results for TOT are presented in Fig. 7c. According to the graph, TOT of NT and TW70 samples was less than 20% in spectral area above 550 nm. In the same visible area, TOT noticeably increased for TW100 and TW135 samples, reaching the values between 70 to 80%. The TOT for TW170 showed high values throughout the whole visible EM spectral area, from 45% at 400 nm to above 80% at about 600 nm light wavelength (Fig. 7c). Apart from the lignin, light absorption also depends on the wood species, wood density, volume of cellulose fraction, orientation of cellulose fibres, and sample thickness (Li *et al.* 2018a).

Relatively small values for DOT and high values for TOT indicate that a lot of transmitted light consisted of scattered photons. Therefore, transparent wood samples are characterized by high values of the haze (Fig. 7d). The values of the haze predominantly depend on wood microstructure (Zhu *et al.* 2016a,b). The haze values were high in the whole visible spectrum for the NT and for TW70 samples. to the light wavelength, the haze values of TW170 samples ranged from 25 to 45%.

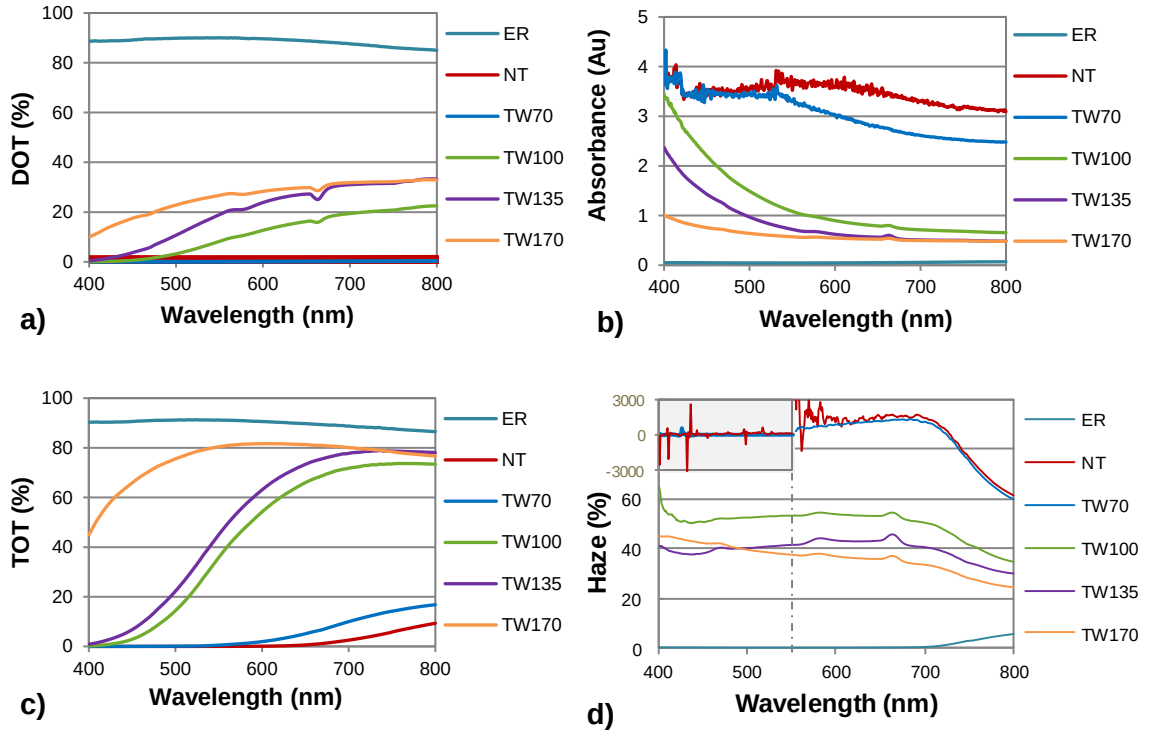

Fig. 7. (a) DOT, (b) absorbance, (c) TOT, and (d) haze of epoxy resin (ER), untreated (NT), and treated samples impregnated with epoxy resin in visible area of EM spectrum (400 to 800 nm)

With prolongation of the treatment duration and increase of delignification degree, the values of haze noticeably decreased. A corresponding decrease in the haze values with decreased lignin content indicates that presence of lignin along with absorbance also affected the amount of the haze. The refraction index value for cellulose and hemicelluloses, which is approximately 1.53 (Li *et al.* 2017a), is close to refraction index of epoxy resin that is 1.50. However, the presence of lignin, with a refraction index of 1.61 (Li *et al.* 2017a) elucidates the higher values of diffraction angle and contributes to the greater scatter of light on its way through the wood cell walls and on the cell wall-epoxy resin boundary surface. Therefore, it is possible that the increase of delignification degree altered optical properties of transparent wood, reducing light scatter and the haze (Fig. 7d).

High values of the optical transmittance and the haze are favorable for employment of transparent wood in civil engineering, allowing natural light in interiors, and providing privacy at the same time (Li *et al.* 2018a). Moreover, the scattering effect could be suitable for solar cells application. Due to the scattering effect through the wood tissue, the light passes through a longer path, allowing better interaction with active medium, thus increasing solar cells' efficiency. It was found that after placing transparent wood on the solar cell active surface increased its efficiency 18.0% (Zhu *et al.* 2016b).

Unlike wood samples, all optical properties of the epoxy resin were almost constant throughout the whole visible EM spectral range. Direct and TOT reached high and almost even values (85 to 90%) in the visible spectral range (Fig. 7a and 7c) whilst the absorbance values of light was negligible (Fig. 7b). Almost the same values for DOT and TOT indicate that the epoxy resin transmitted light with approximately no scattering, which is obvious from the measured values of the haze that are insignificant (Fig. 7d). The presented optical properties of epoxy resin, with which wood was impregnated, had no effect on optical

properties of the wood samples. This indicates that only the physical and chemical structure of wood was responsible for absorption and scattering of light.

CONCLUSIONS

1. A 20% hydrogen peroxide treatment led to delignification of wood. The degree of delignification depended on the treatment duration. The high values of mass loss indicated a certain amount of polysaccharide decomposition along with delignification and extractives dissolution. During the treatment, the cell structure of wood was entirely preserved.
2. Visual assessment of treated samples indicated that prolonged treatment caused lighter color and increased transmittance.
3. The voltage generated on the photo-element, which was proportional to the intensity of monochromatic light that was transmitted through the samples, increased with increased treatment duration, correlating with the lignin content in the samples. Deviations in voltage generated on the photo-element for narrowed and expanded monochromatic light passing through the same samples corresponded to different number of boundary surfaces between cell walls and epoxy resin that the light beam encounters on its way. Great difference in values of generated voltage at different points of the same sample originated from anisotropy in microstructure of wood, as well as different degrees of delignification.
4. The direct optical transmittance (DOT) of visible light for the samples increased as treatment duration was extended. The DOT for all samples was approximately 50% less than the total optical transmittance (TOT), suggesting that a great part of transmitted light originated from scattered photons.
5. High values of the haze for all samples could be attributed to large light dissipation caused by wood microstructure and presence of lignin component, which has a higher value of refraction index than other wood tissue constituents.

REFERENCES CITED

ASTM D1003-00 (2000). "Standard test method for haze and luminous transmittance of transparent plastics," ASTM International, West Conshohocken, PA, USA.

ASTM D1107-96 (1996). "Standard test method for ethanol-toluene solubility of wood," ASTM International, West Conshohocken, PA, USA.

ASTM D2393-86 (1986). "Standard test method for viscosity of epoxy resins and related compounds," ASTM International, West Conshohocken, PA, USA.

Azzam, A. M. (1989). "Pretreatment of cane bagasse with alkaline hydrogen peroxide for enzymatic hydrolysis of cellulose and ethanol fermentation," *Journal of Environmental Science and Health, Part B: Pesticides, Food Contaminants, and Agricultural Wastes* 24(4), 421-433, DOI: 10.1080/03601238909372658.

Bodirlau, R., and Teaca, C. A. (2009). "Fourier transform infrared spectroscopy and thermal analysis of lignocellulose fillers treated with organic anhydrides," *Romanian Journal of Physics* 54(1-2), 93–104.

Dyer, T. J. (2004). *Elucidating the Formation and Chemistry of Chromophores During Kraft Pulping*, Ph.D. Dissertation, Institute of Paper Science and Technology, University of Wisconsin-Stevens Point, Stevens Point, WI, USA.

Faix, O. (1992). "Fourier transform infrared spectroscopy," in: *Methods in Lignin Chemistry*, S. Y. Lin, and C. W. Dence (eds.), Springer Berlin Heidelberg: Berlin, Heidelberg, Germany, pp. 83-109.

Fengel, D., and Wegener, G. (1984). *Wood: Chemistry, Ultrastructure, Reactions*, Walter de Gryter, Berlin, Germany, pp. 133-148.

Fu, Q., Yan, M., Jungstedt, E., Yang, X., Li, Y., and Berglund, L. A. (2018). "Transparent plywood as a load-bearing and luminescent biocomposite," *Composites Science and Technology* 164, 296-303, DOI: 10.1016/j.compscitech.2018.06.001

Gan, W., Gao, L., Xiao, S., Zhang, W., Zhan, X., and Li, J. (2016). "Transparent magnetic wood composites based on immobilizing Fe_3O_4 nanoparticles into a delignified wood template," *Journal of Materials Science* 52(6), 3321-3329. DOI: 10.1007/s10853-016-0619-8

Gan, W., Xiao, S., Gao, L., Gao, R., Li, J., and Zhan, X. (2017). "Luminescent and transparent wood composites fabricated by poly(methyl methacrylate) and γ-Fe_2O_3@YVO_4:Eu^{3+} nanoparticle impregnation," *ACS Sustainable Chemistry & Eng*ineering 5(5), 3855-3862. DOI: 10.1021/acssuschemeng.6b02985

Gelbrich, J., Mai, C., and Militz, H. (2012). "Evaluation of bacterial wood degradation by Fourier-transform-infrared (FTIR) measurements," *Journal of Cultural Heritage* 13(3), S135-S138. DOI: 10.1016/j.culher.2012.03.003

Gellerstedt, G. (2007). "Bleaching chemistry and post-color formation in kraft pulps (Keynote lecture)," in: *3rd International Colloquium on Eucalyptus Kraft Pulp*, Belo Horizonte, Brazi, pp. 1-13.

Gould, J. M. (1984). "Alkaline peroxide delignification of agricultural residues to enhance enzymatic saccharification," *Biotechnology and Bioengineering* 26(1), 46-52. DOI: 10.1002/bit.260260110

Hill, C. A. S. (2006). *Wood Modification: Chemical, Thermal and Other Processes*, John Wiley & Sons, New York, NY, USA.

Kalliola, A., Kuitunen, S., Liitiä, T., Rovio, S., Ohra-aho, T., Vuorinen, T., and Tamminen, T. (2011). "Lignin oxidation mechanisms under oxygen delignification conditions. Part 1. Results from direct analyses," *Holzforschung* 65, 567-574, DOI: 10.1515/hf.2011.101

Lang, A. W., Li, Y., De Keersmaecker, M., Shen, E., Österholm, A. M., Berglund, L., and Reynolds, J. R. (2018). "Transparent wood smart windows: Polymer electrochromic devices based on poly(3,4-ethylenedioxythiophene): Poly(styrene sulfonate) electrodes," *ChemSusChem* 11(5), 854-863. DOI: 10.1002/cssc.201702026

Lewis, I. R, Daniel, Jr., N. W, Chaffin, N. C., and Griffiths, P. R. (1994). "Raman spectrometry and neural networks for the classification of wood types," *Spectrochimica Acta Part A: Molecular and Biomolecular Spectroscopy* 50(11), 1943-1958.

Li, T., Zhu, M., Yang Z., Song, J., Dai, J., Yao, Y., Luo, W., Pastel, G., Yang, B. and Hu, L. (2016a). "Wood composite as an energy efficient building material: Guided sunlight transmittance and effective thermal insulation," *Adv. Energy Mater*. 6(22), article ID 1601122. DOI: 10.1002/aenm.201601122

Li, Y., Fu, Q., Yu, S., Yan, M., and Berglund, L. (2016b). "Optically transparent wood from a nanoporous cellulosic template: Combining functional and structural

performance," *Biomacromolecules* 17(4), 1358-1364. DOI: 10.1021/acs.biomac.6b00145

Li, Y., Fu, Q., Yang, X., and Berglund, L. (2017a). "Transparent wood for functional and structural applications," *Philosophical Transactions A* 376(2112), article ID 20170182. DOI: 10.1098/rsta.2017.0182

Li, Y., Fu, Q., Rojas, R., Yan, M., Lawoko, M., and Berglund, L. (2017b). "A new perspective on transparent wood: Lignin – retaining transparent wood," *A Journal of ChemSusChem* 10(17), 3445-3451. DOI: 10.1002/cssc.201701089

Li, Y., Yu, S., Veinot, J. G. C., Linnros, J., Berglund, L., and Sychugov, I. (2017c). "Transparent wood: Luminescent transparent wood," *Advanced Optical Materials* 5(1), article ID 1600834. DOI: 10.1002/adom.201600834

Li, Y., Vasileva, E., Sychugov, I., Popov, S., and Berglund, L. (2018). "Optically transparent wood: Recent progress, opportunities, and challenges," *Advanced Optical Materials* 6(14), article ID 1800059. DOI: 10.1002/adom.201800059

Li, Y., Yang, X., Fu, Q., Rojas, R., Yan, M., and Berglund, L. (2018b). "Towards centimeter thick transparent wood through interface manipulation," *Journal of Materials Chemistry A*. 6(3), 1094-1101. DOI: 10.1039/C7TA09973H

Lionetto, F., Del Sole, R., Cannoletta, D., Vasapollo, G., and Maffezzoli, A. (2012). "Monitoring wood degradation during weathering by cellulose crystallinity," *Materials* 5(10), 1910-1922. DOI: 10.3390/ma5101910

Miron, J., and Ben-Ghedalia, D. (1982). "Effect of hydrolysing and oxidizing agents on the composition and degradation of wheat straw monosaccharides," *European J. Applied Microbiology and Biotechnology* 15(2), 83-87. DOI: 10.1007/BF00499511

Moosavinejad, S. S., Madhoushi, M., Rasouli, D., and Vakili, M. (2016). "Non-destructive evaluation of wood chemical compounds used in Gorgan historical building *via* FT-IR spectroscopy," *Journals of Wood and Forest Science and Technology* 23(1), 313-328.

Naumann, D., Labischinski, H., and Giesbrecht, P. (1991). "The characterization of microorganisms by Fourier transform infrared spectroscopy (FTIR)," in: *Modern Techniques for Rapid Microbiological Analysis*, W. H. Nelson (ed.), Wiley-VCH, New York, NY, USA, pp. 43–96.

Pandey, K. (1999). "A study of chemical structure of soft and hardwood and wood polymers by FTIR spectroscopy," *Journal of Applied Polymer Science* 71(12), 1969-1975. DOI:10.1002/(SICI)1097-4628(19990321)71:12<1969::AID-APP6>3.0.CO;2-D

Pandey, K. K., and Pitman, A. J. (2003). "FTIR studies of the changes in wood chemistry following decay by brown-rot and white-rot fungi," *International Biodeterioration & Biodegradation* 52(3), 151-160. DOI: 10.1016/S0964-8305(03)00052-0

Pucetaite, M. (2012). *Archaeological Wood from the Swedish Warship Vasa Studied by Infrared Microscopy*," Master's Thesis, Lund University Press, Lund, Sweden.

Ramos, E., Calatrava, S. F., and Jiménez, L. (2008). "Bleaching with hydrogen peroxide. A review," *AFINIDAD LXV* 537, 366-373.

Rowell, R. M. (2005). *Handbook of Wood Chemistry and Wood Composites*, CRC Press, Boca Raton, FL, USA.

Selig, M. J., Vinzant, T. B., Himmel, E. M., and Decker, S. R. (2009). "The effect of lignin removal by alkaline peroxide pretreatment on the susceptibility of corn stover to purified cellulolytic and xylanolytic enzymes," *Applied Biochemistry and Biotechnology* 155, 397-406. DOI: 10.1007/s12010-008-8511-x

Sjöström, E. (1993). *Wood Chemistry; Fundamentals and Application*, 2nd Edition, Academic Press, Inc., San Diego, CA, USA.

Stevanović-Janežić, T. (1993). *Hemija Drveta sa Hemijskom Preradom. Deo 1. Hemija Drveta [Wood Chemistry with Chemical Processing. Part 1. Wood Chemistry]*, Jugoslavijapublik, Belgrade, Serbia.

TAPPI T222 om-02 (2006). "Acid-insoluble lignin in wood and pulp," TAPPI Press, Atlanta, GA, USA.

TAPPI T264 cm-97 (2002). "Preparation of wood for chemical analysis," TAPPI Press, Atlanta, GA, USA.

Traoré, M., Kaal, J., and Martínez Cortizas, A. (2018). "Differentiation between pine woods according to species and growing location using FTIR-ATR," *Wood Science and Technology* 52, 487-504, DOI: 10.1007/s00226-017-0967-9

Tribulová, T., Kacík, F., Evtuguin, D., and Cabalová, I. (2016). "Assessment of chromophores in chemically treated and aged wood by UV-vis diffuse reflectance spectroscopy," *Cellulose Chemistry and Technology* 50(5-6), 659-667.

Wang, L., Liu, Y., Zhan, X., Luo, D., and Sun, X. (2019). "Photochromic transparent wood for photo-switchable smart window applications," *Journal of Materials Chemistry C* 7(28), 8649-8654. DOI: 10.1039/c9tc02076d

Yaddanapudi, H. S., Hickerson, N., Saini, S., and Tiwari, A. (2017). "Fabrication and characterization of transparent wood for next generation smart building applications," *Vacuum* 146, 649-654, DOI: 10.1016/j.vacuum.2017.01.016

Yu, Z., Yongji, Y., Yao, J., Zhang, L., Chen, Z., Gao, Y., and Luo, H. (2017). "Transparent wood containing Cs_xWO_3 nanoparticles for heat-shielding window applications," *Journal of Materials Chemistry A* 5(13), 6019-6024, DOI: 10.1039/C7TA00261K

Zhang, L., Wang, A., Zhu, T., Chen, Z., Wu, Y., and Gao, Y. (2020). "Transparent wood composites fabricated by impregnation of epoxy resin and W-doped VO_2 nanoparticles for application in energy-saving windows," *ACS Applied Materials & Interfaces* 12(31), 34777-34783. DOI: 10.1021/acsami.0c06494

Zhu, M., Song, J., Li, T., Gong, A., Wang, Y., Dai, J., Yao, Y., Luo, W., Henderson, D., and Hu, L. (2016a). "Highly anisotropic, highly transparent wood composites," *Advanced Materials* 28(26), 5181-5187. DOI: 10.1002/adma.201600427

Zhu, M., Li, T., Davis, C. S., Yao, Y., Dai, J., Wang, Y., AlQatari, F., Gilman, J. W., and Hu, L. (2016b). "Transparent and haze wood composites for highly efficient broadband light management in solar cells," *Nano Energy* 26, 332-339. DOI: 10.1016/j.nanoen.2016.05.020

Zhuang, J., Li, M., Pu, Y., Ragauskas, A. J., and Yoo, C. G. (2020). "Observation of potential contaminants in processed biomass using Fourier transform infrared spectroscopy," *Applied Sciences* 10(12), article no. 4345. DOI: 10.3390/app10124345

Article submitted: March 30, 2022; Peer review completed: July 11, 2022; Revisions accepted: August 25, 2022; Published: September 1, 2022.
DOI: 10.15376/biores.17.4.5919-5935